

## Spatial Variations in the Superconductivity of Nb<sub>3</sub>Sn Measured by Low-Temperature Tunneling Microscopy

A. L. de Lozanne, S. A. Elrod, and C. F. Quate

*Department of Applied Physics, Stanford University, Stanford, California 94305*

(Received 25 February 1985)

The low-temperature scanning tunneling microscope is used in a new spectroscopic mode to obtain real-space images of the superconducting character of a Nb<sub>3</sub>Sn surface. These images show strong spatial variations, with reproducible transitions between fully normal and fully superconducting behavior on length scales as small as 13 nm. Images taken above and below the critical temperature confirm that the observed effects are due to superconductive tunneling. Additional confirmation comes from a successful fit of the current-voltage characteristics to a simple tunneling model.

PACS numbers: 73.40.Gk, 68.25.+j, 73.60.Ka

The technique of scanning tunneling microscopy<sup>1</sup> has recently been demonstrated at low temperature.<sup>2</sup> The low-temperature tunneling microscope (LTTM) has the potential for studying the electronic properties of surfaces with a lateral resolution approaching atomic dimensions. In this Letter we report the first images of spatial variations of superconductivity on length scales as small as 13 nm. Poppe and Schroder<sup>3</sup> have developed a similar tunneling apparatus, showing good tunneling characteristics, but to date no scanning (i.e., microscopy) capability has been demonstrated.

Other techniques have been used to study the spatial variations of superconducting properties. Gross *et al.*<sup>4</sup> have used an electron beam to drive a small region of the sample normal while measuring the change in the electrical characteristics. This gives an *indirect* measure of the variations of superconductivity with a resolution that has been demonstrated to 10  $\mu\text{m}$ . This resolution is limited by the thermal healing length, and therefore depends on material parameters and geometrical details. The maximum resolution with this technique is expected to be  $\sim 0.2 \mu\text{m}$ . A similar approach by Chi, Loy, and Cronmeyer<sup>5</sup> uses patterned laser beams while making the same *macroscopic* electrical measurements. The demonstrated resolution is 5  $\mu\text{m}$  and the ultimate limit is  $\sim 0.5 \mu\text{m}$ . While this technique has been used to separate the effects of spatial variations of the superconducting gap from those of the tunneling probability in a macroscopic tunnel junction,<sup>6</sup> the measurement is indirect, limited in resolution, and requires that a tunnel junction be made over the sample. The LTTM provides a *direct* measure of the superconducting gap (via tunneling) with a resolution that is higher than any expected spatial variations.

Here, we describe a technique which exploits the sensitivity of the LTTM to provide full real-space images of the superconducting character of a Nb<sub>3</sub>Sn surface. With the apparatus previously described,<sup>2</sup> the voltage applied across the tunneling junction is triangle-wave modulated at 1 kHz. The analog time

derivative of the junction current is displayed as a function of junction voltage, yielding a sensitive measure of the electronic structure. The 1-kHz sweep rate is fast compared to the response time of the feedback circuit which controls the large-bias ( $V \gg \Delta$ ) gap resistance. Therefore, current-voltage characteristics ( $I$ - $V$ 's) obtained by this method correspond to fixed gap spacing. As shown in Fig. 1(b), the observed superconducting gap of Nb<sub>3</sub>Sn gives rise to the expected zero-bias dip in conductivity, approximated in our case by  $(dI/dt)_{v=0}$ . As the tip is scanned laterally, the magnitude of  $(dI/dt)_{v=0}$  changes both with variations in superconductivity and with topography. Hence, some care must be taken to sort out the different effects on the tunneling current.

In this experiment, we wish to extract a single parameter from the  $I$ - $V$  which is a direct measure of the local superconductivity, but which excludes the effects of changing topography. We accomplish this by sampling the zero-bias value of  $dI/dt$  and normalizing it to  $dI/dt$  at large bias. Through a series of analog operations, this yields a signal which equals unity for normal-insulator-normal metal junctions (independent of topography) and zero for ideal superconductor-insulator-normal metal (SIN) junctions at  $T=0$ . The legitimacy of this technique for normalizing out the topographic features relies on the assumption that the basic physics of the tunneling process and hence the shape of the  $I$ - $V$  curve remains unchanged as the gap resistance varies around its equilibrium value. In this experiment, the large-bias gap resistance ( $V \gg \Delta$ ) was feedback stabilized at 250 k $\Omega$ ; the instantaneous value during scans ranged between 100 and 625 k $\Omega$ .

We recognize that this imaging technique provides an incomplete measure of the local superconductivity; the detailed physics will be fully elucidated only by a quantitative analysis of the  $I$ - $V$  at every point on the surface. The technique described here is intended to give a first view of microscopic variations in the super-

conductor, and to allow one to target particular areas for a more quantitative treatment.

In this experiment, an iridium tip was used to minimize the oxide contribution to the tunneling barrier. The sample was a thin film of  $\text{Nb}_3\text{Sn}$  with a critical temperature of 18 K. In order to reduce the possibility of lattice damage from the cleaning procedure, the sample was not ion-beam cleaned as in a previous experiment,<sup>2</sup> but rather was briefly etched in a 10% aqueous solution of HF 15 min before being pumped down in the vacuum station.

Once the outer walls of the ultrahigh-vacuum cryostat had been cooled to 4.2 K,  $5 \times 10^{-4}$  Torr of He exchange gas was introduced into the vacuum space. Cold-plate baffles ensured that only He gas reached the sample. Tunneling measurements were made in the exchange gas.

To obtain stable  $I$ - $V$ 's, an *in situ* tip-cleaning procedure was required. With  $-30$  V applied to the tip, the tunneling gap spacing was reduced until current flowed. Initially, the current would increase uncontrollably, reaching the resistor-limited value of  $1.2 \mu\text{A}$ .

After several attempts, it became possible to control the current at 200 nA. Images taken after this procedure showed markedly enhanced reproducibility and stability. The tip-cleaning procedure resulted in the extinction of superconductive tunneling over the full field of view of the scanner ( $207 \times 207 \text{ nm}^2$ ). It was therefore necessary to move the tip to a new location with the magnetic positioner<sup>2</sup> in order to observe superconducting features. Occasionally, the topography at the tip-cleaning site showed a mound, indicating that material (Ir) had been transferred from the tip, perhaps by melting. This would explain the extinction of superconductivity at this and nearby sites.

Prior to cleaning of the tip, the  $I$ - $V$ 's were unstable, with gross tunneling features which were superimposed on the less pronounced superconducting gap. Maxima and minima in  $dI/dt$  at voltages from 0 to 100 mV, along with either sign of overall second derivative, were observed. We believe that these effects are caused by resonant tunneling through moving atoms or molecules on the tip or the sample, a phenomenon studied extensively by field emission.<sup>7</sup>

Shown in Fig. 1 are repeated spectroscopic line scans over a region of the sample. They show a continuous spatial transition between superconducting and nearly normal regions which occurs over 23 nm. This is larger than, and therefore consistent with, the coherence length of  $\text{Nb}_3\text{Sn}$  ( $\sim 4 \text{ nm}$ ).  $I$ - $V$ 's for locations I and II are shown in the figure, as is the time derivative used to obtain the spectroscopic signal. The  $I$ - $V$ 's are of much higher quality than those reported previously,<sup>2</sup> resulting from improvements in the system electronics.

Figure 2 shows an  $I$ - $V$  curve taken at a sufficiently low frequency to make phase-lag effects negligible. The fit by a simple SIN tunneling model calculated at the measured temperature is also shown, yielding a fitted value of 2.8 mV for the superconducting gap. The quality of the fit gives us confidence that this is indeed a tunneling process.

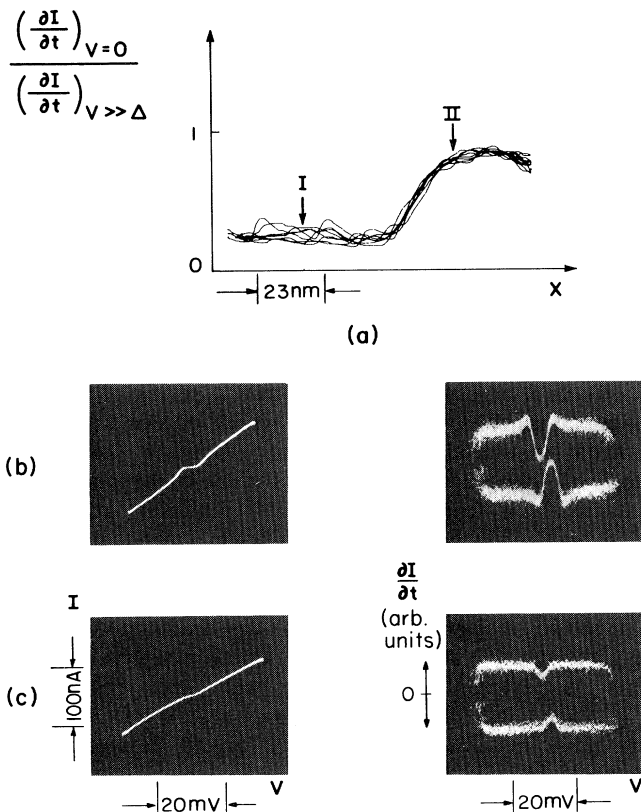


FIG. 1. (a) Repeated spectroscopic (normalized zero-bias conductance) line scans over a region of the  $\text{Nb}_3\text{Sn}$  sample, showing a continuous spatial transition between normal and superconducting behavior. (b),(c)  $I$ - $V$ 's corresponding to locations I and II.

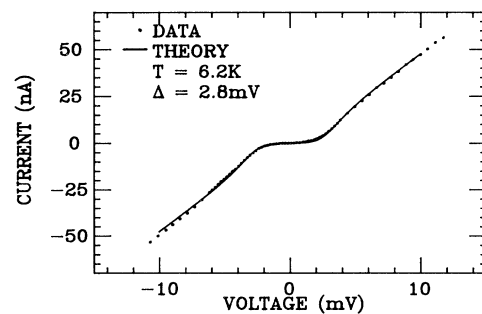


FIG. 2. Comparison of an observed  $I$ - $V$  (points) to a simple temperature-dependent SIN tunneling model (solid line).

Shown in Fig. 3 is a full  $X$ - $Y$  image of the spatial variations of superconductivity over a region of the  $\text{Nb}_3\text{Sn}$  surface. For this image, scanning was in the  $X$  direction; each  $X$  line scan was taken 20 times and the signal averaged by computer. Images taken in immediate succession show excellent reproducibility; rotation of the scanning direction by 90 degrees did not alter the image appreciably. Also shown in the figure is a topographic image taken at the same time. The spectroscopic image shows a transition between normal and superconducting regions which is defined by an arc in the  $X$ - $Y$  plane. The topographic image shows a similar boundary between the two regions; the superconducting region appears topographically flat, while the normal region shows more texture. Possible explanations for observed variations will be discussed below. We note that a significant fraction of our images do not show such variations, but rather show exclusively superconducting or normal behavior.

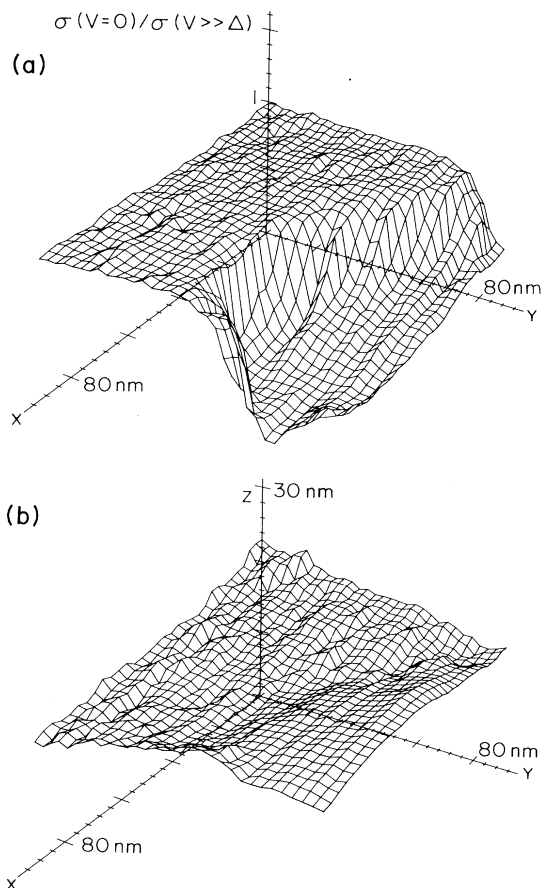


FIG. 3. (a) Full  $X$ - $Y$  images of the superconducting character of the  $\text{Nb}_3\text{Sn}$  sample. The distance between successive grid lines is 2.7 nm. The vertical axis is the normalized zero-bias conductance, as discussed in the text. (b) Topographic data taken at the same time.

Figure 4 shows spectroscopic images taken over a region of the sample below and above its critical temperature. Taken at 6.2 K, Fig. 4(a) shows a distinct transition between normal and superconducting regions. Warming the sample above 20 K with a resistive heater results in the spectroscopic image shown in Fig. 4(b). This figure demonstrates the success of the spectroscopic signal extraction technique in the normalizing out of topographic variations.

We have considered several possible origins of the spatial variations of superconductivity in this sample. The first is microscopic inhomogeneities on a scale of less than  $1 \mu\text{m}$ . This possibility is suggested by heat-capacity measurements<sup>8</sup> which show a spread in the transition temperature of Nb-Sn samples in the composition range of 20 to 24 at.% Sn. Such inhomogeneities are below the lateral resolution of microprobe analysis. Our sample ( $\sim 25$  at.% Sn) is, however, in the composition range which shows a sharp heat-capacity transition. One might therefore naively conclude that it is completely homogeneous. It should be noted, however, that the heat-capacity measurement pertains to the entire thin film, while a tunneling measurement is surface sensitive. Thus it is possible that there are inhomogeneities on the surface which are not present in the rest of the film. This hypothesis is supported by the fact that even the best planar tunnel junctions made on stoichiometric  $\text{Nb}_3\text{Sn}$

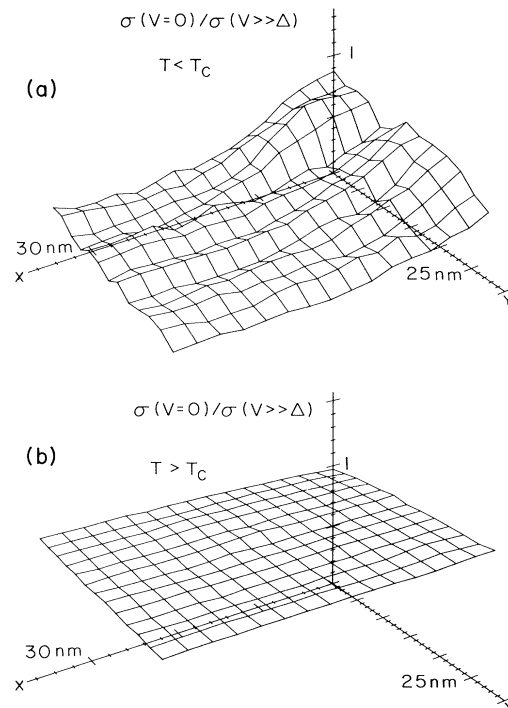


FIG. 4. Spectroscopic images taken (a) below and (b) above the critical temperature.

still show a large spread in the gap (2.3 to 4.1 mV)<sup>9</sup> despite a sharp heat-capacity transition. The origin of this spread is not understood.

The second possibility is gap anisotropy,<sup>10</sup> which would introduce spatial variations due to the different orientations of neighboring microcrystals. Unfortunately, this does not explain a full variation between normal and superconducting regions as shown in Fig. 3. Furthermore, these films typically grow with a preferred [200] orientation normal to the substrate,<sup>9</sup> which means that tunneling proceeds along that direction unless there is enough texture on the surface to allow tunneling in directions other than normal to the substrate.

The last possibility is that the variations are due to damage created either by previous ion milling<sup>2</sup> or by the tip-cleaning procedure described above. This is perhaps the most likely current explanation, since we have found superconductive tunneling to be locally extinguished after tip cleaning, as explained above. The surface roughness on the normal region of Fig. 3 could be an indication of this damage.

The questions of microscopic inhomogeneities and gap anisotropy in the *A*-15 materials are very important in elucidating the mechanism of superconductivity in these high- $T_c$  materials. We believe that once the technical details of obtaining clean, undamaged surfaces are addressed, the LTTM will provide important information on these problems. It should be emphasized that regardless of the cause for the variations observed in this sample, the results demonstrate a direct measurement of the superconducting gap on a scale of two to three orders of magnitude finer than previous techniques. This makes the LTTM a very promising tool not only to study superconducting surfaces but also possibly to obtain microscopic chemical analysis by inelastic<sup>11</sup> or resonant tunneling spectroscopy.

We acknowledge useful discussions with M. R. Beasley and F. Hellman. This work was supported by the Office of Naval Research and by a grant from the Research Division of the IBM Corporation. One of us (S.A.E.) is supported as an Office of Naval Research Fellow while the other (A.L.de L.) is a recipient of a Marvin Chodorow fellowship in applied physics.

---

<sup>1</sup>G. Binnig, H. Rohrer, Ch. Gerber, and E. Weibel, *Phys. Rev. Lett.* **50**, 120 (1983).

<sup>2</sup>S. Elrod, A. L. de Lozanne, and C. F. Quate, *Appl. Phys. Lett.* **45**, 1240 (1984).

<sup>3</sup>U. Poppe and H. Schroder, in *Proceedings of the Seventeenth International Conference on Low Temperature Physics, Karlsruhe, West Germany, 1984*, edited by U. Eckern *et al.* (North-Holland, Amsterdam, 1984), p. 835.

<sup>4</sup>R. Gross, M. Koyanagi, H. Seifert, and R. P. Huebener, in *Proceedings of the Seventeenth International Conference on Low Temperature Physics, Karlsruhe, West Germany, 1984*, edited by U. Eckern *et al.* (North-Holland, Amsterdam, 1984), p. 431.

<sup>5</sup>C. C. Chi, M. M. T. Loy, and D. C. Cronmeyer, *Phys. Rev. B* **29**, 4908 (1984).

<sup>6</sup>M. Scheuermann and C. C. Chi, *Phys. Rev. B* **31**, 4676 (1985).

<sup>7</sup>J. W. Gadzuk, *Phys. Rev. B* **1**, 2110 (1970).

<sup>8</sup>F. Hellman, D. A. Rudman, S. R. Early, and T. H. Geballe, *Bull. Am. Phys. Soc.* **27**, 347 (1982).

<sup>9</sup>D. Rudman, Ph.D. thesis, Stanford University, 1982 (unpublished); D. A. Rudman, F. Hellman, R. H. Hammond, and M. R. Beasley, *J. Appl. Phys.* **55**, 3544 (1984).

<sup>10</sup>*Anisotropy Effects in Superconductors*, edited by H. W. Weber (Plenum, New York, 1977).

<sup>11</sup>*Tunneling Spectroscopy*, edited by P. K. Hansma (Plenum, New York, 1982).

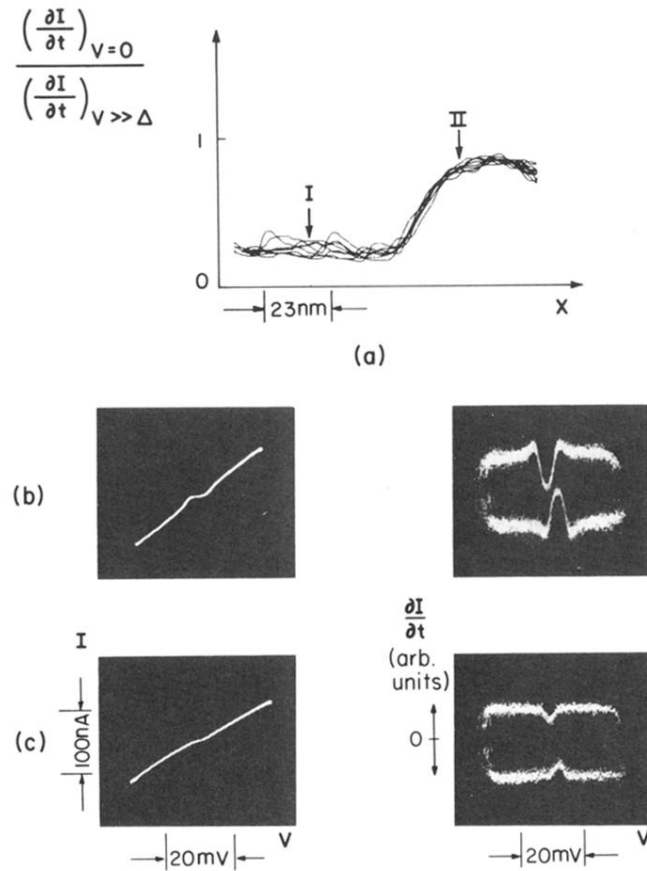


FIG. 1. (a) Repeated spectroscopic (normalized zero-bias conductance) line scans over a region of the  $\text{Nb}_3\text{Sn}$  sample, showing a continuous spatial transition between normal and superconducting behavior. (b),(c)  $I$ - $V$ 's corresponding to locations I and II.